

## Qualitative and Quantitative Monitoring of Methyl Cotton Biodiesel Content in Biodiesel/Diesel Blends Using MIR Spectroscopy and Chemometrics Tools

José Eduardo Buiatte,<sup>a</sup> Eloíza Guimarães,<sup>a</sup> Hery Mitsutake,<sup>a</sup> Lucas Caixeta Gontijo,<sup>\*,a,b</sup>  
Douglas Queiroz Santos<sup>c</sup> and Waldomiro Borges Neto<sup>a</sup>

<sup>a</sup>Instituto de Química, Universidade Federal de Uberlândia, Campus Santa Mônica,  
38408-100 Uberlândia-MG, Brazil

<sup>b</sup>Instituto Federal Goiano de Educação, Ciência e Tecnologia, 75790-000 Urutaí-GO, Brazil

<sup>c</sup>Escola Técnica de Saúde, Universidade Federal de Uberlândia, Campus Umuarama,  
38400-902 Uberlândia-MG, Brazil

This paper presents methodologies for monitoring the quality of methyl cotton biodiesel in biodiesel/diesel blends using mid-infrared spectroscopy (MIR) and chemometrics tools. The first method relates to the construction of multivariate control charts with the aim of qualitatively monitoring the samples according to the Brazilian specification for biodiesel in the biodiesel/diesel blends ( $7.00 \pm 0.5\%$  v/v of biodiesel). The second concerns the construction of partial least squares (PLS) to determine the content of the biodiesel in the biodiesel/diesel blend. The PLS model was validated from multivariate figures of merit according to the guidelines of ASTM E1655-05 and IUPAC. The results from both methods were satisfactory for both qualitative and quantitative monitoring. Therefore, the proposed methodologies for monitoring the quality of biodiesel in biodiesel/diesel blends are fast, practical, economical and efficient and can be used by industries and service stations.

**Keywords:** biodiesel, mid-infrared spectroscopy, chemometrics tools, multivariate control charts, PLS

### Introduction

The search for alternatives to oil use increases the importance of commercial production of biofuels.<sup>1</sup> Among the biofuels, biodiesel has stood out for being a renewable fuel derived from vegetable oils, animal fats or waste, and can be a total or partial surrogate of mineral diesel.

Thus, in 2005, this fuel was introduced to the Brazilian energy matrix<sup>2</sup> and the addition of 7% (v/v) to diesel oil has now become mandatory.<sup>3</sup> Therefore, due to the requirement of this blend, analytical control of the biodiesel content blended with diesel is critical. Biodiesel production in Brazil can use various feedstocks (any oilseed and animal fats) and various alcohols (usually methanol or ethanol), provided that the final product meets the specifications of the National Agency of Petroleum, Natural Gas and Biofuels (ANP).<sup>4</sup> Thus, the choice of raw material depends on the availability, cost and production technology.<sup>5</sup> In this

perspective, considering that about 50-90% of biodiesel production costs is due to the raw material used, the use of oils derived from waste has been excelled, as this decreases the cost of production.<sup>6,7</sup> Therefore, cottonseed oil becomes a viable oilseed because it is a waste of cotton production. Moreover, it is the third most commonly used raw material in biodiesel production in Brazil and the country is the fifth largest producer of cotton.<sup>8</sup>

Diverse methodologies for the study of the quality of biodiesel in biodiesel/diesel blend are designed, involving various techniques and combined with some types of chemometric tools. Among such techniques are near infrared spectroscopy (NIR)<sup>9</sup> and mid-infrared spectroscopy (MIR),<sup>10,11</sup> high-performance liquid chromatography (HPLC),<sup>12</sup> mass spectrometry with electrospray ionization (ESI-MS)<sup>13</sup> and others.<sup>14,15</sup> However, most studies have been developed with respect to soybean biodiesel, or to separate the produced biodiesel from different sources. No studies to monitor the quality of this biofuel in blends with diesel using multivariate control charts or regression partial least

\*e-mail: quilucas10@gmail.com

squares (PLS) methodologies from MIR spectroscopy data have been found.

In this context, this paper presents multivariate methodologies for the identification and quantification of methyl cotton biodiesel content in biodiesel/diesel blends using mid-infrared spectroscopy.

#### Brief description of multivariate control charts based on NAS

Control charts consists of charts that monitor some important feature of a quality control process. The charts based on net analytical signal (NAS) allow separate control, but simultaneous analysis of the quality of the analyte of interest and its mother, who is not modeled by either of these two (noise/waste).<sup>16</sup>

The basis for the development of control charts is shown in Figure 1, in which a sample spectrum (vector  $\mathbf{r}$ ) is divided into three different contributions: the NAS vector ( $\mathbf{r}_{\text{NAS}}$ ) for monitoring the analyte of interest, the interference vector ( $\mathbf{r}_{\text{int}}$ ) and the residual vector ( $\mathbf{r}_{\text{res}}$ ). The contributions related to the analyte of interest (biodiesel in the case of this study) are modeled by the NAS vector; the contributions of the matrix (diesel) are modeled by interference vector and the contributions that were not modeled by NAS and interference vectors correspond to the residual vector.<sup>17</sup> From the statistical limits calculated for each contribution/vector, it is possible to determine whether a sample is within the quality compliance or not. Thus, a sample is considered under control, i.e., within quality specifications, if it is within all the calculated limits; otherwise, if it protrudes from at least one of the thresholds, the sample is considered out the quality specifications (out of control). Limits of NAS chart are calculated from the standard deviation of the mean NAS and the 95% confidence limit. The interference projection vectors are calculated for the spectra of the interfering area, as shown in Figure 1. The distance of this projection relative to the ellipse center provides the

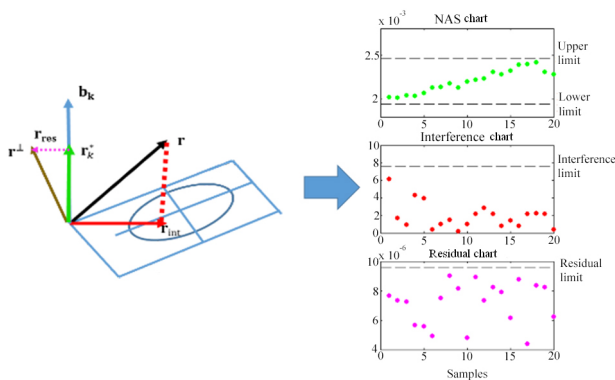


**Figure 1.** The instrumental signal decomposition in three different contributions: NAS vector ( $\mathbf{r}_{\text{NAS}}$ ) for monitoring the analyte of interest, the interference vector ( $\mathbf{r}_{\text{int}}$ ) and the residual vector ( $\mathbf{r}_{\text{res}}$ ).

distance value  $D$ , which is used to compute the threshold of the interference chart 95% reliability. The limits of the residual chart are calculated based on the  $\chi^2$  statistics of the sum of squares of the residual vector of the calibration samples.<sup>16</sup> The equations for calculating the boundaries of three charts can be found in the literature.<sup>16-18</sup>

#### Brief description of PLS

Partial least squares regression (PLS) is a chemometric tool that is widely used in multivariate calibration in various fields of science. In the PLS modeling, both the matrix of independent variables  $\mathbf{X}$  and the dependent variables  $\mathbf{Y}$  are represented by scores and weights according to equations 1 and 2.

$$\mathbf{X} = \mathbf{T}\mathbf{P}^t + \mathbf{E} \quad (1)$$

$$\mathbf{Y} = \mathbf{U}\mathbf{Q}^t + \mathbf{F} \quad (2)$$

where  $\mathbf{X}$  is the matrix of data (measurement instrument),  $\mathbf{Y}$  is the vector response (concentration, for example),  $\mathbf{T}$  and  $\mathbf{U}$  are the scores for the two data matrices,  $\mathbf{P}$  and  $\mathbf{Q}$  are the respective weights,  $\mathbf{E}$  and  $\mathbf{F}$  are the respective residues, or matrices containing the part that is not modeled. The relationship between the two data arrays  $\mathbf{X}$  and  $\mathbf{Y}$  can be obtained by correlating the scores of each block, to obtain a linear relationship described in equation 3.

$$\mathbf{U} = \mathbf{b}\mathbf{T} + \mathbf{e}\mathbf{E} \quad (3)$$

where  $\mathbf{U}$  is a matrix containing the properties of all samples (in this case, the concentration),  $\mathbf{b}$  is a vector containing the model parameters,  $\mathbf{T}$  is a response matrix (spectra) for the calibration samples, and  $\mathbf{E}$  is a matrix representing the spectrum of the noise and model errors.<sup>19</sup>

In this process, the choice of the number of latent variables is necessary, which is usually done by using a so-called cross-validation procedure based on the lowest prediction error. Evaluating the reliability of the constructed model for the validation can be done according to ASTM E1655-05<sup>20</sup> or by figures of merit such as: accuracy, linearity, selectivity, sensitivity, analytical sensitivity, limit of detection, limit of quantification, signal to noise ratio, and test to systematic error (bias), including confidence ellipse.

## Experimental

### Biodiesel production

Ten lots of diesel-free biodiesel used in sample preparation was ceded by Transpetro S/A. The cottonseed

oil, used in the biodiesel synthesis was acquired by Triângulo Alimentos S/A industry. To obtain biodiesel, 30 g of methyl alcohol, 1 g of KOH and 100 g of oil in a molar ratio (1:6) were used. Methyl alcohol-KOH manual agitation was used until complete homogenization, forming the potassium methoxide. The oil was added to the methoxide for 80 min at room temperature and stirred using a magnetic stirrer. At the end of the reaction, there was phase separation in which the glycerin was removed and the biodiesel was washed with hot water to remove impurities. The biodiesel drying step was carried out using a rotary evaporator for 1 h at 78 rpm and 80°C.

### Sample preparation

For the construction of control charts, the following samples divided into five sets were prepared, I: 10 diesel samples free of biodiesel; II: 20 samples under control (6.5-7.5%, v/v) used in the calibration set which were used to determine the limits of statistical control charts (this variation of concentration was chosen due to variation in the volume allowed by Resolution 50 ANP,<sup>21</sup> i.e., 0.5% v/v the percentage of biodiesel in the blend); III: 10 samples under control (6.5-7.5%, v/v) used in the validation set, we used to determine the statistical limits of the charts; IV: 16 biodiesel samples whose concentrations are below the allowed and ranged from 0.5 to 6.0% (v/v); V: 12 samples with biodiesel content is above specified and varied 8.0-14.0% (v/v). The weight measurements were performed on an analytical balance (Sartorius, BP211D model). The solutions were homogenized on a vortex shaker (Phoenix, AP56 model). From the weight and density values of biodiesel and diesel the volume/volume relations were determined. In the construction of the PLS model, samples were prepared by adding biodiesel to ten lots of diesel fuel in a concentration range of 1.00% to 30.00% (v/v). Samples concentrations of 1 to 10% (v/v) were prepared in increments of 0.25%, 10 to 25% (v/v) in increments of 0.75% and after 25% (end of calibration curve) increments of 0.25% (v/v). The samples used for calibration (46 samples) and prediction (27 samples) were prepared on the model so that the prediction concentrations were different concentrations of the calibration.

### Acquisition of spectral data

The MIR spectra were obtained in five replications in the region of 4000 cm<sup>-1</sup> to 600 cm<sup>-1</sup> using the SpectrumTwo model spectrometer (Perkin Elmer) with the horizontal attenuated total reflectance (HATR) ZnSe crystal attachment (Pike Technologies). Control charts for the pre-processing

of data were made by first derivative. For the PLS model, baseline treatment was applied by the baseline function in the regions 1850-2570 cm<sup>-1</sup> and 3200-4000 cm<sup>-1</sup>. To execute the multivariate procedures, MATLAB software version 6.1 (Mathworks Inc.) and PLS\_Toolbox, version 3.5 (Eigenvector Research) were used.

## Results and Discussion

Figure 2 shows the MIR spectra of diesel and methyl cotton biodiesel. The diesel spectrum has substantial absorption bands corresponding to characteristic vibrational modes of normal alkanes. There are three significant absorption spectral regions: (i) the region between 2840 cm<sup>-1</sup> and 3000 cm<sup>-1</sup> attributed to axial deformation vibration of C-H bond of methyl and methylene groups; (ii) intermediate intensity bands in the region of 1300 cm<sup>-1</sup> to 1500 cm<sup>-1</sup> derived from the angular deformation vibration of the C-H bond of methylene and methyl group; and (iii) low intensity band, which is relevant in the region of 720 cm<sup>-1</sup>, resulting from the asymmetric angular deformation vibration of C-H deformations of methylene grouping. When analyzing the spectrum of biodiesel, in addition to the characteristic vibrational modes of methyl groups and methylene, two strong bands are observed: (i) stretching of C=O bonds in the region 1700 cm<sup>-1</sup> to 1750 cm<sup>-1</sup> and (ii) axial vibrations in the region of C=O bond 1100 cm<sup>-1</sup> to 1300 cm<sup>-1</sup>.<sup>22</sup>

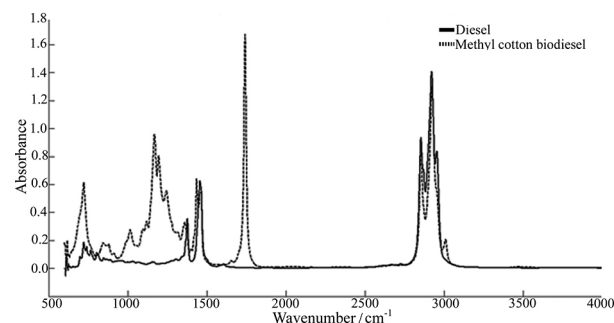
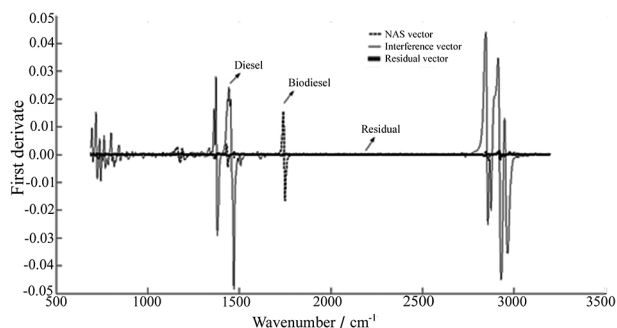


**Figure 2.** Mid-infrared spectra of diesel and methyl cotton biodiesel.

For control charts, various mathematical treatments were tested. The best result was obtained using the first derivative because showed better performance in the correct classification of samples. The derivative was performed to remove baseline effects and to emphasize the spectral differences in each sample. The intervening space was built from the decomposition by principal component analysis (PCA) of the spectra of 10 samples of pure diesel (group I). Three principal components (PC) were chosen, which explained 100.00% of the variance. The statistical limits were calculated from the vectors NAS, interference

and residual, arising from the decomposition of the spectra of the calibration samples (group II).

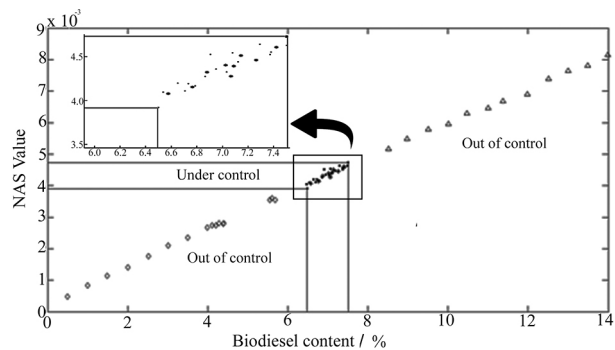
It can be observed in Figure 3 that the most intense signals is the interference vector (diesel) for being the largest percentage component in the blend, i.e., much higher than the concentration of the analyte of interest, biodiesel. The regions in which the NAS vectors have higher intensities than the interference vectors are in  $1760\text{--}1730\text{ cm}^{-1}$  and  $1000\text{--}1300\text{ cm}^{-1}$ . These regions refer to absorptions due to C=O and C–O bands stretching present in the biodiesel, respectively. Moreover, it is observed that the residual vectors have low intensity demonstrating that small amount of the spectral signal is not modeled by the NAS and interference vectors.



**Figure 3.** Intensity of NAS, interference and residual vectors obtained from the calibration samples.

The vector NAS (biodiesel) is directly proportional to analyte concentration. Figure 4 shows the NAS vector in relation to the percentage of biodiesel in samples under control (groups II and III) and out of control (group IV: content below 6.5% and group V: content above 7.5%). The good linearity observed in Figure 4 demonstrates the linear relationship between the NAS vector and the concentration of biodiesel.

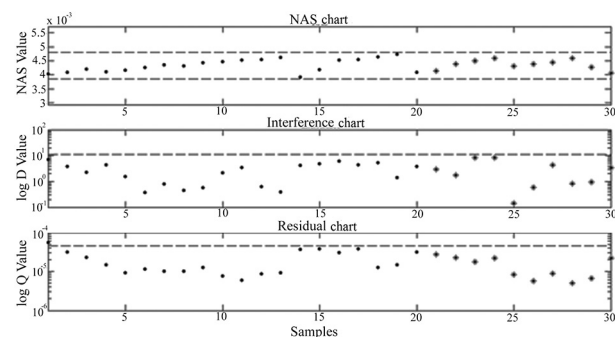
After the spectral decomposition step, the confidence limits were calculated for each chart using only samples



**Figure 4.** Relationship between the NAS vector and biodiesel concentration. (●) group II (calibration set: under control); (\*) group III (validation set: under control); (◇) group IV and (△) group V: out of control samples.

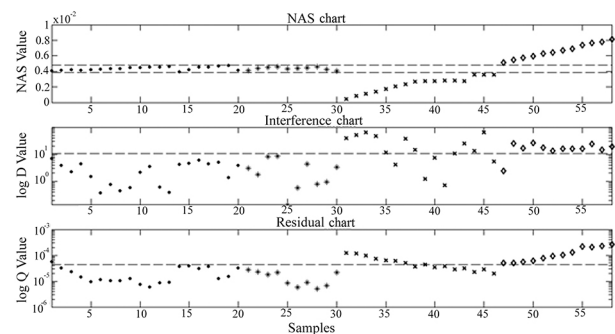
under control. The upper limit ( $NAS_{\text{superior}}$ ) was 0.0048 and the lower ( $NAS_{\text{inferior}}$ ) was 0.0039. The limits obtained for interference chart ( $D_{\text{limit},95\%} = 10.8597$ ), showed values higher than those found for the other charts. This is because these vectors have a much higher intensity than the NAS vectors. In relation to the residual limit ( $Q_o$ ), the value found was  $4.4733 \times 10^{-5}$ , considering that this determination was from samples under control, and that these samples that are not modeled by NAS and interference vectors are very small spectral parts, it was expected that the limits found for these charts were much lower than those found for the NAS and interference charts.

Figure 5 shows the control charts obtained for the calibration (group II) and validation (group III) samples. The first sample of the calibration set was erroneously classified as out of control because it came out of limit of residual chart. A possible explanation for this is that may have occurred an unexpected variation in the spectrometer signal or even an error in the preparation of this sample. However, all other samples were considered correctly as under control.



**Figure 5.** Multivariate control chart for the samples under control, where (●) group II and (\*) group III.

Figure 6 shows the multivariate control chart for the samples out of control because they have less than 6.5% (group IV) and more than 7.5% (group V) of biodiesel. The group IV values were below the lower limit, while



**Figure 6.** Multivariate control charts for the samples out of control, where (x) group IV (18 samples with 0.5 to 6.0% biodiesel) and (◇) group V (12 samples from 8.0 to 14.00% of biodiesel).

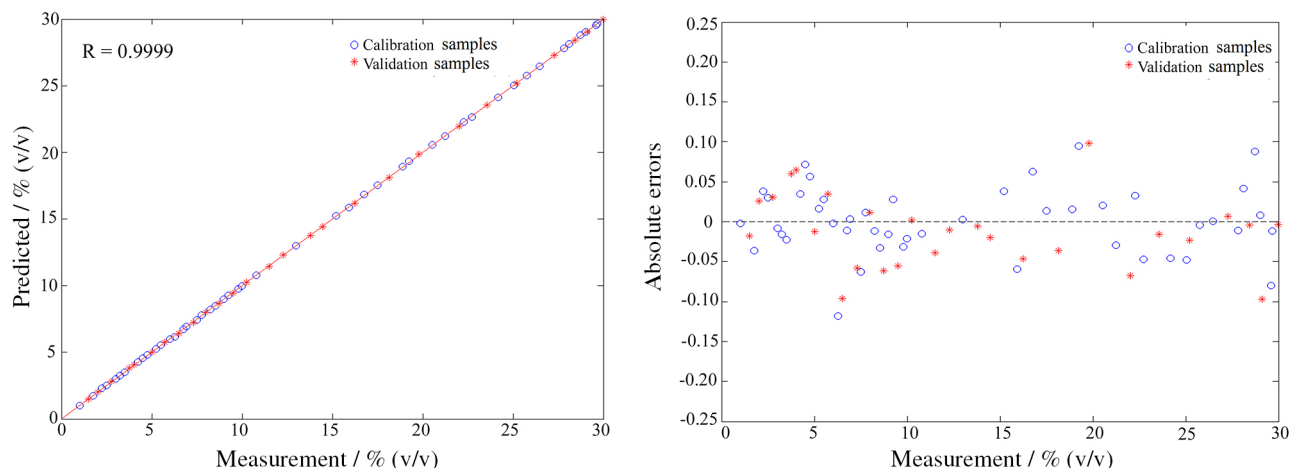


**Figure 7.** In (a) fit of the PLS models through the real *versus* predicted values of the prediction set. In (b) PLS residuals for the calibration and prediction set for the methyl cotton biodiesel in biodiesel/diesel blends.

group V samples show NAS values above the upper limits, as expected due to the property of the NAS to be proportional to the concentration of the analyte of interest in the sample. Thus, all samples of groups IV and V were properly monitored as out of control, demonstrating that this methodology is effective for the monitoring of quality biodiesel in biodiesel/diesel blends.

The PLS model was built using three latent variables which explained 99.96% and 99.99% of the variance of blocks **X** and **Y**, respectively. The presence of outlier was evaluated by Q residuals *versus* leverage, and it was found that no sample was considered an outlier. After this evaluation, it was shown that the number of samples used in the construction of the PLS model was in accordance with the guidelines of ASTM E1655-05.<sup>20</sup>

The fit of the model (Figure 7a) was evaluated by correlating the reference values and the values calculated by the model of the calibration and prediction sets. It was found that both sets (calibration and validation) showed low dispersion with respect to the expected values, i.e., regression coefficient (R) greater than 0.99. However, the value of R alone was not sufficient to confirm linearity, meaning that it is also necessary to analyze the plot of residuals for calibration and prediction samples. Thus, the Figure 7b shows that the proposed models exhibit linear behavior, since the distribution of residuals follows a random pattern.

Table 1 shows the results of figures of merit for the PLS model. The accuracy of the model was evaluated in terms of root mean square error of calibration (RMSEC), root mean square error of cross validation (RMSECV) and root mean square error of prediction (RMSEP). Low error values indicate that the values estimated by the PLS model have good agreement with the reference values. The model also has a value of RMSEP below 0.1%, which is within the allowed by the standard NBR 15568.<sup>23</sup>

**Table 1.** Results of the parameters of figures of merit for the PLS model

Figures of merit	Value
RMSEC / % (v/v)	0.05
RMSECV / % (v/v)	0.04
RMSEP / % (v/v)	0.05
Limit of detection / % (v/v)	0.08
Limit of quantification / % (v/v)	0.25
Selectivity	0.26
Sensitivity / % (v/v) <sup>-1</sup>	0.10
Analytical sensitivity / % (v/v)	40.22
Inverse of analytical sensitivity / (v/v) <sup>-1</sup>	0.02
$t_{\text{calculated}}$	1.3750
$t_{\text{critical}}$	2.0210

However, the evaluation of the model accurately from just the RMSEP value comprises all kinds of errors, both systematic and random. Thus, another way to compare the actual values and the predicted values is from the elliptical joint confidence region (EJCR) with respect to intercept and slope obtained from the regression of actual and projected values. Thus, it is observed in Figure 8 the point (1.0) lies inside the EJCR showing that the actual and predicted values do not present a significant difference with 95% confidence, that is, the absence of systematic errors.<sup>24,25</sup>

The presence of systematic errors was also evaluated according to the t test described by ASTM E1655-05.<sup>20</sup> The results in Table 1 show that the calculated value  $t$  ( $t_{\text{calculated}} = 1.3750$ ) is smaller than the critical value ( $t_{\text{critical}} = 2.0210$ ) with 95% confidence, which indicates that the influence of the systematic errors can be negligible, i.e., the values predicted by the PLS model essentially provide the same average result as the actual values.<sup>20</sup>

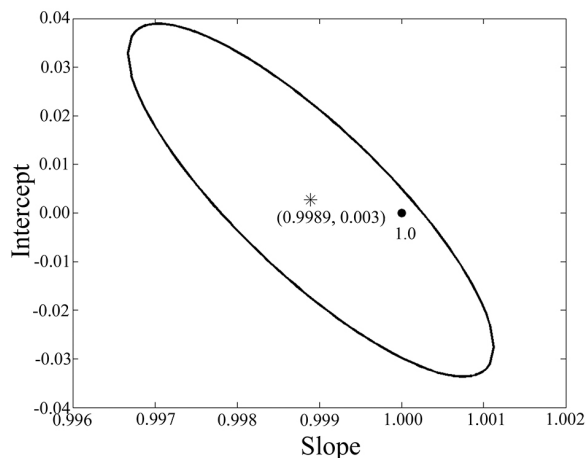


**Figure 8.** The elliptical joint confidence region (EJCR) for the slope and intercept of the regression of predicted concentration versus the reference values. The ideal result consisting of intercept = 0 and slope = 1 is shown by point (●), whereas the experimental result corresponding to intercept = 0.003 and slope = 0.9989 is indicated by asterisk (\*).

Sensitivity was estimated as  $0.10\% \text{ (v/v)}^{-1}$  (Table 1). This parameter expresses an increase in the signal fraction when the concentration of the analyte of interest has a high value for one unit.<sup>26</sup> The inverse of the analytical sensitivity value, shown in Table 1, can be interpreted more clearly because of the direct relationship with the concentration. According to this value, the PLS model is able to distinguish differences among samples with concentration in the range of  $0.02\% \text{ (v/v)}$ .

The selectivity parameter had a value of 0.26, indicating a significant overlap of the interfering signal with the analyte. However, unlike the univariate methods where there is a need for highly selective methods to perform the analysis, multivariate methods are employed in the construction of models from non-selective signals, where the application effectively selects information extracted from these data.<sup>27</sup> Moreover, a major advantage of the PLS is its ability to determine the analyte of interest, even in the presence of interferences, since these are present in the calibration.

By evaluating the limit of detection and the limit of quantification of the PLS model (Table 1), it was verified that the PLS model could detect amounts of biodiesel in diesel above  $0.08\% \text{ (m/m)}$ , while for the quantification, the model could not determine values lower than  $0.25\% \text{ (m/m)}$ . As the concentration of biodiesel in the proposed PLS model ranges from  $1.00\%$  to  $30.00\% \text{ (m/m)}$ , the model is effective at detecting and quantifying biodiesels in diesel blends at concentrations higher than  $0.25\% \text{ (m/m)}$ .

## Conclusion

The methodology developed from MIR spectroscopy data combined with chemometric tools enables the monitoring of

methyl cotton biodiesel content in both the qualitative and quantitative aspects. Control charts can improve the quality of diagnoses, once out of control samples are easily identified in relation to the amount of biodiesel in the blend. It is simple, fast and can be developed for on-line monitoring sensors, requiring only the MIR spectra of samples under control and blank samples to build the charts. The development of the PLS model derived from data MIR blends of biodiesel/diesel fuel was also successful, indicating that the methodology can be applied to the quantification of methyl cotton biodiesel blended with diesel in the range of  $1.00$  to  $30.00\% \text{ (v/v)}$ . Validation of the PLS model was performed according to ASTM E1655 and Brazilian and international validation guides. The model developed is simpler than that proposed by ABNT NBR 15568, with the creation of a single curve for the concentration range of  $1.00$  to  $30.00\% \text{ (v/v)}$  and without the use of solvents, as well as being within the error permitted by this standard. Therefore, regulators and supervisory bodies to control the biodiesel content in blends with diesel can use this methodology.

## Acknowledgements

The authors would like to thank CAPES and FAPEG for their financial support and Caramuru S/A and Transpetro S/A for supplying the samples of the fuel.

## References

1. The United States Pharmacopeia, USP 34-NF 29, The United States Pharmacopeial Convention: Rockville, 2011.
2. Kwon, E. E.; Jeon, E. C.; Yi, H.; Kim, S.; *Appl. Energy* **2014**, *116*, 20.
3. Ministério de Minas e Energia, Lei No. 11097, Diário Oficial da União: Brasília, 2005.
4. Ministério de Minas e Energia, Lei No. 13033, Diário Oficial da União: Brasília, 2014.
5. National Agency of Petroleum, Natural Gas and Biofuels; *Resolution ANP No. 14*; Diário Oficial da União: Brasília, 2012.
6. Pinho, D. M. M.; Santos, V. O.; dos Santos, V. M. L.; Oliveira, M. C. S.; da Silva, M. T.; Piza, P. G. T.; Pinto, A. C.; Rezende, M. J. C.; Suarez, P. A. Z.; *Fuel* **2014**, *136*, 136.
7. Huang, Y. P.; Chang, J. I.; *Renewable Energy* **2010**, *35*, 269.
8. Joshi, H.; Moser, B. R.; Walker, T.; *J. Am. Oil Chem. Soc.* **2011**, *89*, 145.
9. Associação Brasileira dos Produtores de Algodão; *Report 2014*. Available at: <http://www.abrapa.com.br/estatisticas/Paginas/Algodao-no-Brasil.aspx> accessed in September 2015.
10. Balabin, R. M.; Safieva, R. Z.; *Anal. Chim. Acta* **2011**, *689*, 190.
11. Gontijo, L. C.; Guimarães, E.; Mitsutake, H.; de Santana, F. B.; Santos, D. Q.; Borges Neto, W.; *Fuel* **2014**, *117*, 1111.

11. Mazivila, S. J.; de Santana, F. B.; Mitsutake, H.; Gontijo, L. C.; Santos, D. Q.; Borges Neto, W.; *Fuel* **2015**, *142*, 222.
12. Brandão, L. F. P.; Braga, J. W. B.; Suarez, P. A. Z.; *J. Chromatogr. A* **2012**, *1225*, 150.
13. Eide, I.; Zahlsten, K.; *Energy Fuel* **2007**, *21*, 3702.
14. Corgozinho, C. N.; Pasa, V. M.; Barbeira, P. J.; *Talanta* **2008**, *76*, 479.
15. Meira, M.; Quintella, C. M.; Tanajura, A. S.; da Silva, H. R. G.; Fernando, J. D. S.; da Costa Neto, P. R.; Pepe, I. M.; Santos, M. A.; Nascimento, L. L.; *Talanta* **2011**, *85*, 430.
16. Skibsted, E. T. S.; Boelens, H. F. M.; Westerhuis, J. A.; Smilde, A. K.; Broad, N. W.; Rees, D. R.; Witte, D. T.; *Anal. Chem.* **2005**, *77*, 7103.
17. de Oliveira, I. K.; Rocha, W. F. C.; Poppi, R. J.; *Anal. Chim. Acta* **2009**, *642*, 217.
18. Rocha, W. F. C.; Poppi, R. J.; *Microchem. J.* **2010**, *96*, 21.
19. Vandeginste, B. G. M.; Massart, D. L.; Buydens, L. M. C.; Jong, S.; Lewi, P. J.; Smeyers-Verbeke, J.; *Handbook of Chemometrics and Qualimetrics: Part B*, 1<sup>st</sup> ed.; Elsevier Science: Amsterdam, 1988.
20. ASTM E1655: *Standard Practices for Infrared Multivariate Quantitative Analysis*, West Conshohocken, 2005.
21. National Agency of Petroleum, Natural Gas and Biofuels; *Resolution No. 50*; Diário Oficial da União: Brasília, 2013.
22. Holler, F. J.; Skoog, D. A.; Crouch, S. R.; *Princípios de Análise Instrumental*, 6<sup>a</sup> ed.; Bookman: Porto Alegre, 2002.
23. ABNT NBR 15568: *Biodiesel: Determination of Biodiesel Content in Diesel Oil via Mid-Infrared Spectroscopy*; ABNT: Rio de Janeiro, 2008.
24. de Souza, L. M.; Mitsutake, H.; Gontijo, L. C.; Borges Neto, W.; *Fuel* **2014**, *130*, 257.
25. Valderrama, P.; Braga, J. W. B.; Poppi, R. J.; *J. Agr. Food. Chem.* **2007**, *55*, 8331.
26. Valderrama, P.; Braga, J. W. B.; Poppi, R. J.; *Quim. Nova* **2009**, *32*, 1278.
27. Olivieri, A. C.; Faber, N. M.; Ferré, J.; Boqué, R.; Kalivas, J. H.; Mark, H.; *Pure Appl. Chem.* **2006**, *78*, 633.

Submitted: June 23, 2015

Published online: September 29, 2015